Dispersion-managed solitons in a fiber loop with in-line filtering

E. A. Golovchenko, J. M. Jacob, A. N. Pilipetskii, C. R. Menyuk, and G. M. Carter

Department of Computer Science and Electrical Engineering, University of Maryland, Baltimore County, Baltimore, Maryland 21250

Received October 2, 1996

We investigate both numerically and experimentally soliton propagation in a fiber loop with dispersion management, in-line filters, and frequency shifting. More than 90% of the fiber in the loop is in the normal-dispersion regime, but the net dispersion is anomalous. Stable pulses in the loop have an enhanced power relative to solitons in a fiber with uniform dispersion equal to the loop's path-averaged dispersion. Because the loop's path-averaged dispersion is small, the in-line filtering and the frequency shifting play an important role in pulse shaping. Recirculating loop experiments that demonstrate stable pulse propagation over 28,000 km are consistent with results from computer modeling. © 1997 Optical Society of America

Recent experimental[1] and theoretical[2,3] studies show that dispersion management is a promising approach to improve the performance of soliton transmission systems. Dispersion-managed schemes have the advantage that they can support stable pulse propagation very close to zero-path-averaged group-velocity dispersion (GVD), leading to a reduction in both the Gordon–Haus[4] and the acoustic[4,5] timing jitter. Previous computer simulations have shown that solitons in dispersion maps with large deviations of the local dispersion from the average will have an enhanced power relative to solitons in a fiber with uniform dispersion equal to the path-averaged dispersion of the map,[3] and the stable pulse dynamics along the dispersion map are analogous to stretched pulses in mode-locked fiber lasers.[6] We report an observation of such pulses in a recirculating loop experiment in which more than 90% of the fiber is in the normal-dispersion regime, although its net dispersion is anomalous. A key element of this experiment, as in almost all recirculating loop experiments, is an acousto-optic modulator that allows us to switch out the data periodically for loading and unloading the loop. In doing so, it downshifts the frequency of the signal propagating in the loop. Because our average dispersion is low, this downshift—along with the in-line filters that are required for suppression of amplified spontaneous-emission noise outside the channel bandwidth—play an important role in the pulse shaping. In this Letter we examine this issue both theoretically and experimentally.

The schematic illustration of our recirculating fiber loop is shown in Fig. 1. The loop consists of four fiber spans separated by Er-doped fiber amplifiers. Each of the first three spans consists of a 25-km length of dispersion-shifted fiber with normal GVD, $D_1 = -1.2$ ps/(nm km) at $\lambda = 1.55$ μm. The fourth span consists of a 25-km length of dispersion-shifted fiber connected to a standard fiber with an anomalous GVD, $D_2 = 16.5$ ps/(nm km). We chose the length of the standard fiber so that the average GVD $D = 0.1$ ps/(nm km). The system operated with 25–30-ps pulses that were filtered by a 1.2-nm filter and were frequency shifted 100 MHz by an acousto-optic modulator after each circulation, implying a frequency shift of 1 GHz/Mm.

In our computer model we used input pulses with a duration τ(FWHM) = 25 ps that was equal to the pulse duration in our experiments and a hyperbolic secant shape. We varied the pulse power to find a stable propagation regime. Pulse propagation in the fiber spans was modeled with the nonlinear Shrödinger equation with a loss equal to 0.2 dB/km. We included the third-order dispersion $D' = 0.07$ ps/(nm^2 km) in our computer model. However, in our calculations we did not observe any significant effect from its influence. The amplifier gain at the peak of the filter transmission function was chosen to overshoot the integrated loss of the fiber loop by an amount α, which is referred to as the excess gain.[7] The excess gain, together with the frequency-dependent loss, provides the necessary frequency-dependent balance between gain and loss that allows for stable pulse propagation in filtered systems. The input pulse was injected with its central frequency at the peak of the filter transmission function. In our system the stable pulses are not strict solitons even in an averaged sense; they are entities whose shape varies substantially over one period of the dispersion map but which return to the same shape at the end of each period.

If the filter transmission function is approximated by a parabola, pulse in-line filtering can be described

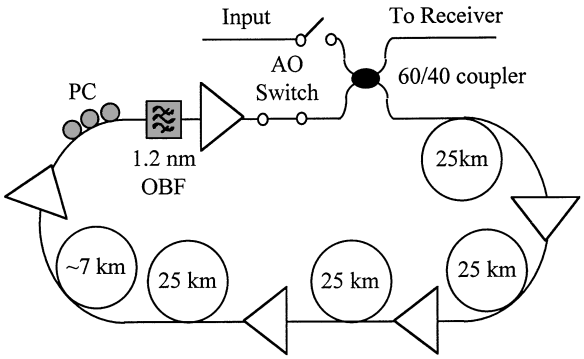

Fig. 1. Experimental setup of the recirculating fiber-optic loop.

0146-9592/97/050289-03$10.00/0

by the expression

$$\frac{\partial u}{\partial z} = \frac{1}{2}\,\frac{\eta}{L_F}\,\frac{\partial^2 u}{\partial t^2}, \tag{1}$$

where u is the complex amplitude of the electric field, $L_F = 108$ km is the filter separation, and η is the curvature at the peak of the filter transmission function. By analogy with the dispersion length $z_d = \tau_0^2 2\pi c/D\lambda^2$, where $\tau_0 = \tau(\mathrm{FWHM})/1.76$, we can now introduce a filtering length $z_F = \tau_0^2 L_F/\eta$. A typical nonlinear scale length in soliton transmission is the soliton period $z_0 = \pi z_d/2$. When the average value of GVD is low, the soliton period becomes comparable with the filtering length z_F, and the filter then plays an important role in pulse shaping. For our parameters the soliton period was $z_0 = 2500$ km, and the filtering length was $z_F = 4350$ km. Similar considerations apply to the frequency shift that we used. The value $f' = 1$ GHz/Mm is almost an order of magnitude smaller than a typical sliding rate in the sliding filters that have been used in soliton transmission experiments,[4] but it is nonetheless large in soliton units.[8] For our parameters the filter strength $\beta = z_d/z_F$ and the frequency-shifting rate $\gamma = 2\pi f' \tau_0 z_d$ in soliton units were $\beta = 0.36$ and $\gamma = 0.14$, respectively. For the stable pulses that are formed in our loop the sliding rate is nearly critical.[7,8]

Figure 2 shows the peak intensity, the pulse width, and the frequency offset versus the transmission distance. The input pulse parameters were the same in all the simulations. It can be seen that, without the filters, the pulses have not reached equilibrium even after 40,000 km but continue to oscillate. With filtering but no frequency shifting the pulses oscillate because of interaction with the amplified, linear dispersive wave, as shown in the middle of Fig. 2 by the dotted curve.[9] The length scale on which this oscillation occurs can, in principle, be lengthened by means of a decrease in the excess gain. In our experiments this instability was canceled out by the frequency shifting. The simulations that include both filtering and frequency shifting are shown in Fig. 2 as the dotted and the dotted–dashed curves. In this case pulses reach a stable equilibrium after just 5000–8000 km. At this equilibrium the pulses stretch and compress with the periodicity of the loop, returning to a well-defined shape at the end of each period. Depending on the value of the excess gain, either the filter can trap the pulse or the pulse can damp by the system because of insufficient gain. In our experiments the evolution of the intensity of the light pulse along the line was monitored by measurement of the fundamental 8-GHz rf component after the pulse's passage through the photodetector. The circles in Fig. 2 show the experimental dependence of the fundamental 8-GHz rf component versus the transmission distance. The experimental curve is in good agreement with the simulation results. Comparing the pulse parameters with and without filtering and frequency shifting (shown in Fig. 2), we find that frequency shifting, as well as filtering, plays an important role in stablizing the pulses at distances greater than ~8000 km and that the stable filtered

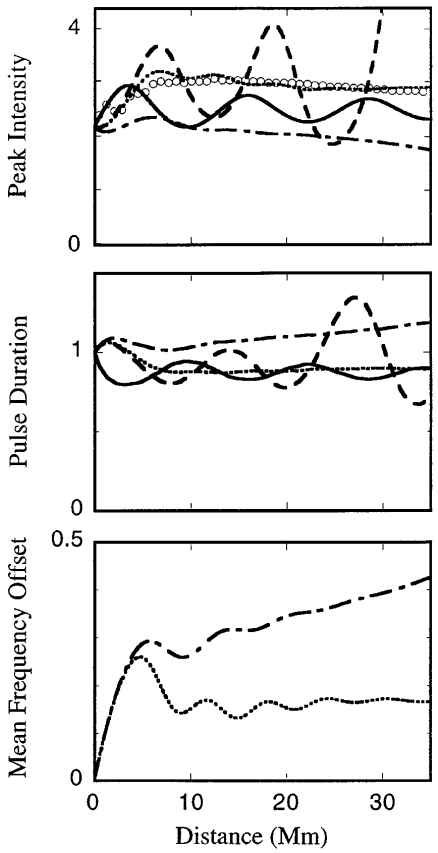

Fig. 2. Calculated evolution of the pulse peak intensity, duration at FWHM, and the absolute value of the pulse mean frequency in the transmission scheme shown in Fig. 1. The input pulse intensity was $I(z = 0) = 2.25I_0$, where I_0 is the intensity of an average soliton. The pulse width is normalized to the input pulse width, and the mean frequency is shown in soliton units. The data are plotted at the last amplifier output after each dispersion map. The solid curve corresponds to the case in which there are no filters, amplifiers, or frequency shifting. The dashed curve corresponds to the loop with in-line filters and amplifiers but no frequency shifting; the excess gain $\alpha = 0.27$. The dotted–dashed curve and the dotted curve correspond to a loop with in-line filters, amplifiers, and frequency shifting; the excess gain is $\alpha = 0.22$ and $\alpha = 0.27$, respectively. The circles show the experimental data for the fundamental 8-GHz rf component.

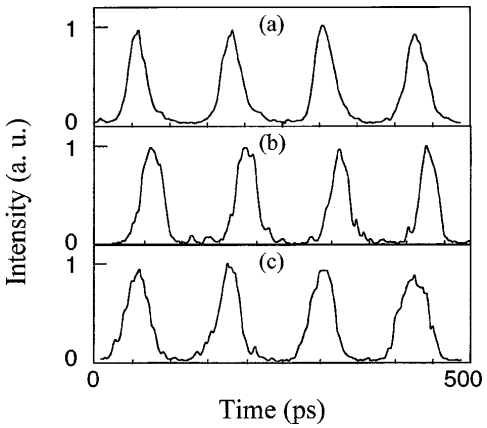

Fig. 3. Experimentally observed 8-GHz optical pulse trains (a) for 0 Mm, (b) at 10 Mm, and (c) at 28 Mm.

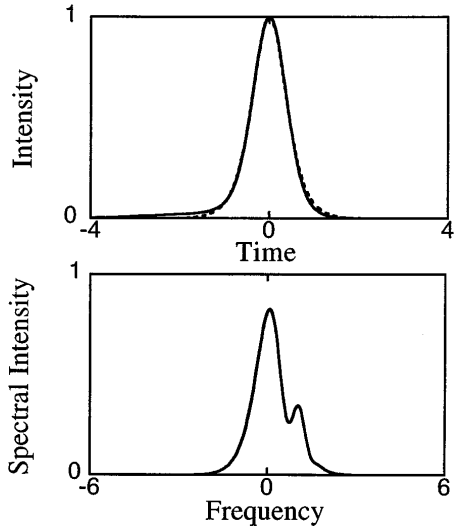

Fig. 4. Calculated stable pulse and spectrum shapes at 40,000 km when the excess gain $\alpha = 0.27$. The dotted curve is the input pulse. The time scale is normalized to the pulse FWHM, and the frequency is shown in soliton units.

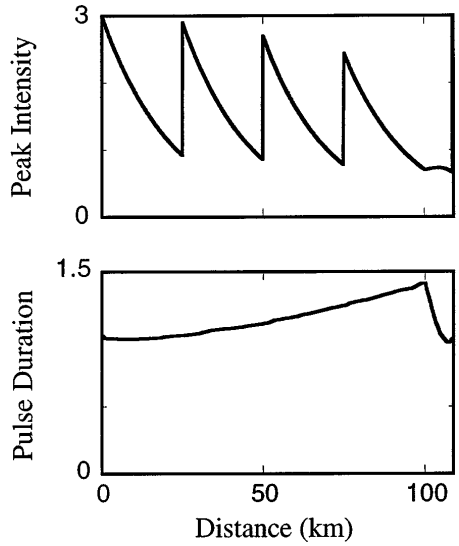

Fig. 5. Calculated evolution of the stable pulse peak intensity, and duration at FWHM inside the dispersion map after the pulse propagated over 40,000 km for the value of the excess gain $\alpha = 0.27$. The previous evolution of the pulse parameters is shown in Fig. 2 by a dotted curve.

pulses, shown by the dotted curve, have ~10% more power resulting from excess gain than do pulses in an unfiltered system with the same duration. At equilibrium the pulses in the computer simulations reproduce their shapes and spectra after each cycle of dispersion management. Figure 3 shows the experimentally observed pulses in the recirculating fiber loop. The pulses stabilized at a distance of ~8000 km, and then they stably propagated, reproducing their shapes or spectra after each loop cycle, consistent with the simulations.

The computer simulations predict that the stable pulse, obtained with filtering and frequency shifting, has an asymmetric shape in time and an asymmetric spectrum, as shown in Fig. 4. However, the detection of this asymmetry is beyond the resolution of our experiments. The calculated stable pulse evolution inside the dispersion map is shown in Fig. 5. The pulses stretch in the positive-GVD part of the map by up to 1.4 times the input duration and compress in the negative-GVD part by as much as the initial duration.

In conclusion, we have studied dispersion-managed soliton propagation in a recirculating fiber loop that is more than 90% in the normal-dispersion regime, although its net dispersion is anomalous. We have investigated the effects of weak filtering and frequency shifting owing to an acousto-optic modulator, and we have found that, at a low value of the path-averaged GVD, these elements play an important role in the pulse shaping. These elements are present in our recirculating loop experiments as in nearly all recirculating loop experiments that have been done to date, and our experiments confirm that with their presence a stable equilibrium is obtained in 5000–8000 km, as was theoretically predicted. Although it is clear that the acousto-optic modulator has a profound effect on the pulse shaping, it is not clear how it affects the bit-error rate performance. To elucidate this point, we anticipate carrying out future experiments in which the frequency shift owing to the acousto-optic modulator is canceled.

Research at the University of Maryland was supported by the National Science Foundation, the U.S. Department of Energy, and the Advanced Research Projects Agency through the U.S. Air Force Office of Scientific Research.

References

1. M. Suzuki, I. Morita, S. Yamamoto, N. Edagawa, H. Taga, and S. Akiba, Electron. Lett. **23,** 2027 (1995).
2. M. Nakazawa and H. Kubota, Electron. Lett. **31,** 216 (1995).
3. N. J. Smith, F. M. Knox, N. J. Doran, K. J. Blow, and I. Bennion, Electron. Lett. **32,** 54 (1996); M. Nakazawa, H. Kubota, A. Sahara, and K. Tamura, IEEE Photonics Technol. Lett. **8,** 1088 (1996).
4. L. F. Mollenauer, P. V. Mamyshev, and M. J. Neubelt, Opt. Lett. **19,** 704 (1994).
5. E. A. Golovchenko and A. N. Pilipetskii, J. Lightwave Technol. **12,** 1052 (1994).
6. H. A. Haus, K. Tamura, L. E. Nelson, and E. P. Ippen, IEEE J. Quantum Electron. **31,** 591 (1995).
7. A. Hasegawa and Y. Kodama, *Solitons in Optical Communications* (Clarendon, Oxford, 1995), pp. 134–139.
8. P. V. Mamyshev and L. F. Mollenauer, Opt. Lett. **19,** 2083 (1994).
9. M. Matsumoto and A. Hasegawa, Opt. Lett. **18,** 897 (1993).